Food & Function

Human gut microbiota-fermented asparagus powder protects human epithelial cells from injury and inflammation

Journal:	*Food & Function*
Manuscript ID	FO-ART-07-2024-003504.R1
Article Type:	Paper
Date Submitted by the Author:	15-Dec-2024
Complete List of Authors:	Rajakaruna, Sumudu; Wright State University, Department of Biochemistry and Molecular Biology Bandow, Brant; Wright State University, Department of Biochemistry and Molecular Biology Pérez-Burillo, Sergio; Wright State University, Department of Biochemistry and Molecular Biology Navajas-Porras, Beatriz; University of Granada, Department of Nutrition and Food Sciences Rufian-Henares, J.; University of Granada, Department of Nutrition and Food Sciences; University de Granada, Instituto de Investigación Biosanitaria ibs.GRANADA Cool, David ; Wright State University, Department of Pharmacology & Toxicology Cho, Kwang-Jin; Wright State University, Department of Biochemistry and Molecular Biology Paliy, Oleg; Wright State University, Department of Biochemistry and Molecular Biology

Human gut microbiota-fermented asparagus powder protects human epithelial cells from injury and inflammation

Sumudu RAJAKARUNA [a], Brant BANDOW [a], Sergio PÉREZ-BURILLO [a], Beatriz NAVAJAS-PORRAS [b], José Ángel RUFIÁN-HENARES [b,c], David R. COOL [d], Kwang-Jin CHO [a], and Oleg PALIY [a*]

[a] *Department of Biochemistry and Molecular Biology, Boonshoft School of Medicine, Wright State University, Dayton, Ohio, USA*

[b] *Department of Nutrition and Food Sciences, Instituto de Nutrición y Tecnología de los Alimentos, Centro de Investigación Biomédica, University of Granada, Granada, Spain*

[c] *Instituto de Investigación Biosanitaria ibs.GRANADA, University de Granada, Granada, Spain*

[d] *Department of Pharmacology & Toxicology, Boonshoft School of Medicine, Wright State University, Dayton, Ohio, USA*

[*] Corresponding author. Address: 260 Diggs Laboratory, Wright State University, 3640 Colonel Glenn Hwy, Dayton OH 45435, USA. Email: oleg.paliy@wright.edu

Author emails:
rajakaruna.2@wright.edu
bandow.3@wright.edu
spburillo@gmail.com
beatriz.navajas@fisabio.es
jarufian@ugr.es
david.cool@wright.edu
kwang-jin.cho@wright.edu
oleg.paliy@wright.edu

Abstract

Dietary consumption of green asparagus has been associated with several health benefits. These beneficial properties are attributed to the presence of many bioactive compounds in asparagus, including saponins, phenolics, flavonoids, as well as dietary fiber mostly comprising fructans and inulins, which are prebiotics capable of supporting the growth of beneficial members of gut microbiota. In this study, we used the *in vitro* Human Gut Simulator system to assess the fermentation of oro-gastro-intestinally digested asparagus powder by the human gut microbiota. Microbial community composition differed between communities grown on the asparagus digest and on the Western diet derived medium. Asparagus supported beneficial *Ruminococcus* but also hydrogen sulfide producing members of Desulfovibrionaceae. Fermentation of asparagus released more antioxidants into the environment compared to the Western diet medium, and supernatant of asparagus-grown cultures protected cultured human epithelial cells against damage and inflammation. We thus showed that asparagus powder has a potential to be used as a functional food, offering protection against intestinal damage and inflammation – effects mediated by the gut microbiota.

Keywords: asparagus, gut microbiota, short-chain fatty acids, antioxidants, human microbiome

Introduction

Asparagus is a perennial herb that has been used as a vegetable since ancient times. Currently, over 200 species of asparagus have been identified, out of which only *Asparagus officinalis* is cultivated as a commercial vegetable in over 60 countries [1]. China, Western Europe, North America, and Peru are the largest asparagus producers, while the USA is the largest importer (accounting for 92,000 tons in 2018) [2]. Fresh or canned asparagus products are utilized in salads, soups, as well as additives in meat or poultry dishes. Recent market predictions indicate that global consumption of asparagus is on an upward trend [2].

Increased popularity of asparagus consumption could be attributed to it being a low caloric food with numerous bioactive compounds as well as due to better availability of asparagus on the market. Green asparagus has higher concentrations of bioactive compounds compared to less popular purple and white varieties of *A. officinalis* and is promoted as one of the healthier foods [3]. Saponins, phenolics, sterols, and flavonoids are considered the main groups of bioactive compounds in asparagus [1]. Among the commonly consumed vegetables, asparagus is among the top ranked with respect to its antioxidant properties. These are attributed to the presence of phenolic phytochemicals such as saponins, rutin, and protodioscin [4]. In addition, asparagus products also exert metal chelating properties, and 2″-

hydroxynicotianamine isolated from asparagus was shown to inhibit the activity of angiotensin-converting enzymes in the kidneys through metal chelation [5]. Asparagus also contains an appreciable amount of dietary fiber, mostly comprising fructans and inulins as well as hemicelluloses and pectins, all of which are not digestible by human oro-gastro-intestinal (OGI) enzymes and are thus available for fermentation by gut microbes [6]. Dietary fiber in asparagus extracts have shown hypoglycemic and hypotriglyceridemic properties, suggesting a potential use of asparagus in the management of diabetes [7]. In addition, asparagus and its products have also been used in medicinal applications due to its purported anti-neurotoxic properties (shown in rats) [8], antitumor properties (shown *in vitro*) [9], blood cholesterol regulation through bile acids binding (shown *in vitro*) [10], and even as a treatment for insomnia in humans [11].

Deviating from the traditional use, novel nutritional trends suggest incorporating dried asparagus powder into the diet. Asparagus moisture content varies in the different parts of the shoots, and this moisture is removed through various drying processes during the commercial production of asparagus powder [1]. Use of asparagus powder in meatloaf preparation has resulted in a novel meat product of high nutritive value, antioxidant activity, and sensory attractiveness [12]. Furthermore, fortification with asparagus powder has been shown to change the physiochemical parameters of cheese and improve its nutritional value [13]. Fiber extracts from asparagus have also been used to enrich yoghurts [14]. Furthermore, the incorporation of asparagus powder in value-added pasta preparations has improved the firmness, hardness, and protein and fiber content of such pasta [15].

Many health benefits of asparagus are attributed to its nutritional composition, where dietary fiber and bioactive compounds such as polyphenols stand out as key contributors. The majority of these phytochemicals escape human OGI digestion and are available to colonic microbiota, which could ferment these compounds and also release bound polyphenols into the gut [16]. However, despite the importance of exploring the benefits of asparagus consumption with respect to gut health, there is little to no extensive work available on how asparagus is fermented by the gut microbiota. In this study, we investigated the OGI digestion and subsequent gut microbiota fermentation of green asparagus powder using the *in vitro* Human Gut Simulator system [17].

Materials and Methods

In vitro digestion of asparagus powder.

Dried asparagus powder from *Asparagus officinalis* (green asparagus) was obtained commercially (Nutricargo LLC, MI). The nutritional composition of asparagus powder was calculated based on the composition of fresh asparagus as 20 calories, 0.1 g total fats, 3.9 g total carbohydrates including 2.1 g

of dietary fiber, and 2.2 g of proteins per 100 grams as listed in the USDA FoodData Central database. These values were adjusted to reflect the content equivalent in dried asparagus powder with 5% moisture, as per industrial asparagus drying protocols. We carried out an *in vitro* digestion of dried asparagus powder designed to mimic the human OGI digestion of foods as was described previously [18]. Briefly, during the oral digestion phase, asparagus powder was mixed with simulated salivary fluid in 1:2 ratio and maintained at 37 ºC for 2 minutes at pH 7, to mimic human oral digestion conditions (see **Figure 1A**). Due to the high hygroscopic nature of the asparagus powder, the use of 1:2 ratio ensured the proper salivary digestion. The generated oral bolus was mixed in 1:1 ratio with the simulated gastric fluid and was maintained at 37 ºC for 2 hours at pH 3. This process was equivalent to the human gastric digestion. Finally, the produced gastric chyme was mixed in 1:1 ratio with the simulated intestinal fluid and maintained at 37 ºC for 2 hours at pH 7 to mimic the human intestinal digestion. This final mixture was centrifuged in 50-ml aliquots at 6,000 rpm, and supernatant and residues were collected, homogenized, and stored at -70 ºC until further use. For enzymatic digestions, pepsin was purchased from Sigma-Aldrich (St Louis, MO), and the enzymatic assay was performed to determine the enzyme activity [19]. Amylase and pancreatin was purchased from MP Biomedicals (Irvine, CA), and the enzymatic activity values were provided by the manufacturer.

In vitro Human Gut Simulator (HGS) experiments.

Gut microbial fermentation of the digested asparagus powder was carried out in the *in vitro* HGS system, which had been previously described and validated [17]. HGS is a fully anaerobic system comprised of five linked compartments: a medium reservoir, a proximal colon vessel, a transverse colon vessel, a distal colon vessel, and a waste collector. The compartments are connected via medium transfer tubes, and medium is transferred by automatically operated peristaltic pumps, which ensure unidirectional movement of contents mimicking the movement of a food bolus in the gut. The medium reservoir contains a nutrient medium that was designed to mimic the contents that reach the gut of an adult after digestion of Western pattern diet foods (called Western diet medium, or WM) [17]. At day 0, each vessel was inoculated with a homogenized fecal inoculum prepared from fresh fecal samples obtained from three healthy adults (male and female North Americans and male Western European; age range 24-43, BMI range 19.3-24.8). Donors were screened for the use of dietary supplements, antibiotics, and history of gastrointestinal diseases within six months prior to stool donation.

Each vessel was volume-, temperature-, and pH-regulated to match the conditions of its respective colonic region, and the contents were mixed continuously. The system was sparged twice daily with a mixture of N_2 and CO_2 gases to ensure anaerobicity. The system was operated continuously

for six weeks. Two replicate runs were performed, with each run comprising three different phases that differed in the composition of medium provided to the proximal vessel (**Table 1** and **Figure 1B**). In phase 1, western diet medium was provided for the first two weeks to establish a stable microbiota community in each region (day 0 to day 14: phase 1) [18, 20]. After two weeks, the medium reservoir was switched to supply the digested asparagus medium (denoted YEM+ASP, **Table 1**) for two more weeks (day 14 to day 28: phase 2). YEM+ASP contained the same salt concentrations as WM. However, all macronutrients of WM (with an exception of yeast extract required to provide vitamins and cofactors) were replaced by asparagus digest residue, which was added in equivalent amount (23.9 g l^{-1}). Additionally, 10% of the digested asparagus supernatant was also added to represent the digested soluble compounds escaping absorption in the small intestine [21]. The yeast extract concentration was similar to WM, and mucin was not added to the YEM+ASP medium because addition of mucin during this phase would add additional nutrients that are not of asparagus origin. During this phase, members of the gut community that are capable of utilizing asparagus bioactive compounds along with syntrophic organisms were expected to thrive. After a further two weeks, the reservoir medium was changed to contain yeast extract medium (YEM) for the final two weeks (day 28 to day 42: phase 3). Compared to the YEM+ASP medium, YEM lacked both the asparagus digest as well as the supernatant, hence YEM provides limited amounts of nutrients, mainly through the yeast extract. Detailed nutrient constituents in each medium are provided in **Table 1**.

Throughout the HGS runs, multiple samples were taken as shown in **Figure 1B**, and cell densities were measured by phase contrast microscopy using a Spencer hemocytometer. Collected samples were centrifuged to separate them into cell pellets, which were used for bacterial genomic DNA isolation using ZR bacterial DNA isolation kit (Zymo Research), and the supernatants, which were used for short-chain fatty acid (SCFA) and antioxidant measurements. All samples were stored at -70 ºC.

Microbiota composition analysis.

Isolated bacterial genomic DNA was amplified in a PCR reaction targeting V4 hypervariable region of the 16S rRNA gene using degenerate forward (16S rRNA gene complementary sequence GCCAGCMGCCGCGG) and reverse (complementary sequence GGACTACHVGGGTWTCTAAT) primers [20]. PCR reaction consisted of 4 linear and 25 exponential cycles in order to reduce PCR amplification biases [20, 22]. Generated amplicons were sequenced on the Ion Torrent Personal Genome Machine using multiple Ion 318 and 316 chips (Thermo Fisher Scientific) as described previously [23]. We obtained an average of 20,916 sequence reads per sample after quality filtering (minimum 11,408, maximum 36,079). Reads were processed in QIIME [24] using our default pipeline, followed by the 16S

copy number adjustment [20, 25]. Taxon annotation was based on the Ribosomal Database Project Classifier v2.11 and RDP 16S rRNA training set 19. Cell counts of all samples were multiplied to match the cell density of each sample [17], and this cell density adjusted dataset was used for all downstream analyses. Cumulative table of genus-level cell densities in all samples is provided in **Supplementary Table S1**.

Calculation of cumulative counts of beneficial and detrimental microbes.

We employed our recently published approach [21] to estimate the total cell counts of microbial taxa considered to be either beneficial or detrimental to human health. Briefly, cell density adjusted taxon counts of predetermined beneficial and detrimental members were summed and their collective counts were expressed as the relative combined abudance of beneficial and detrimental taxa. Total beneficial microbes consisted of combined abundances (arithmetic sum) of *Akkermansia*, *Bifidobacterium*, *Eubacterium*, *Faecalibacterium*, *Lactobacillus*, *Roseburia*, and *Streptococcus*. Total detrimental microbes combined the abundances of *Clostridioles difficile*, Desulfovibrionaceae, Enterobacteriaceae, *Fusobacterium*, and *Helicobacter*.

Short-chain fatty acid measurements.

The preparation of samples for the chromatographic analysis was performed by centrifuging fermentation supernatant samples at 13,300 rpm for 5 min, filtering them through a 0.22 μm pore size filter and performing a 1:10 dilution with 1M hydrochloric acid [26]. SCFAs were resolved by the HPLC analysis on the Agilent Poroshell 120 SB-Aq column (3 x 150 mm, 2.7 μm particle size). The mobile phase was 5 mM sulfuric acid with isocratic elution at a flow rate of 0.5 ml min^{-1}. The injection volume was 5 μl. The column and detector temperature were set at 35 °C.

The chromatographic analysis was performed in duplicate for each sample. Quantification was carried out against calibration curves constructed for the following external standards: acetic, butyric, lactic, isovaleric, propionic, and succinic acids, in concentrations ranging from 0 to 100 mM. Results were expressed in mmol of each acid per liter (mM) of fermentation supernatant.

Antioxidant capacity measurements.

Antioxidant capacity of samples was estimated using an ABTS assay adapted to a microplate reader (FLUOStar Omega, BMG Labtech) as we have done previously [16]. In the assay, 2,2′-azino-bis(3-ethylbenzothiazoline-6-sulfonic acid) diammonium salt (ABTS) is oxidized by potassium persulfate to form an ABTS-radical cation, which has a characteristic blue-green color. The assay measures the

antioxidant capacity of samples to prevent or revert back this oxidation in comparison with a Trolox standard. The reactions combined 280 µl of the working ABTS solution with 20 µl of a sample or Trolox standard in each well of a 96-well polystyrene plate, and the color development was measured spectrophotometrically in triplicates. The Trolox standard curve was constructed by using a range of Trolox concentrations between 0.01 and 0.1 mg ml $^{-1}$, and the obtained results were expressed as mmol (Trolox equivalents) per liter of sample.

Epithelial cell culture experiments.

Human colorectal cancer Caco-2 cells were received from ATCC (Catalog #HTB-37) and were maintained in DMEM medium (Gibco) supplemented with 10% fetal bovine serum (HyClone), 2 mM L-glutamine (GenDepot) and 1x penicillin/streptomycin mixture (Lonza) at 37 ºC in 5% CO_2. For experimental assays, $1x10^5$ cells were seeded in the semipermeable supports (Corning Transwell, 12 mm diameter, 0.45 µm pore size). Cells were maintained for 21 days with replacement of fresh complete growth medium every two days to promote basolateral-apical differentiation. Differentiation was followed by measuring transepithelial electrical resistance (TEER, see below). After 21 days, cells were treated with 5% dextran sulfate sodium (DSS) alone or in combination with the following solutions: SCFA mixture, a WM-grown culture supernatant (day 14), an asparagus digest medium-grown culture supernatant (day 28), and a fresh non-fermented asparagus medium. Control wells contained complete growth medium without DSS. Supernatants and asparagus medium were provided in 1/10 concentrations to account for the expected metabolite gradient from the lumen to the epithelial surface [27]. SCFA mixture contained acetic, butyric, and propionic acids matching the measured concentrations of these acids in the diluted (1/10) asparagus digest medium. After applying treatments, wells were incubated at 37 ºC in 5% CO_2 for 24 hours. For each assay, we performed two independent experiments for each of the two HGS runs, each with duplicates. Out of two replicate wells, one was used for the MTS and TEER assays (see below), while the other well was used for RNA isolation. Thus, four replicate values were obtained for each measurement.

TEER assay measured the current across the epithelial layer and served to assess the epithelial barrier function. Transepithelial resistance was measured with an EVOM^2 instrument (World Precision Instruments) following manufacturer's instructions. To assess the effect of DSS treatment on epithelial barrier function, TEER measurements were recorded in all wells immediately before the treatments, and six and 24 hours after the treatment.

For the MTS assay, cells were trypsinized and counted after 24 h of treatment. A total of 5.0 x 10^4 cells were added in triplicates along with fresh complete growth medium to a 96-well plate, and the

assay was carried out using the CellTiter AQueous Cell Proliferation Assay kit (Promega) following manufacturer's protocol. Colorimetric reaction development was measured after 1h and 3h of incubation at OD_{490nm}.

To measure the expression of select cytokines in the treated epithelial cells, total RNA was isolated from harvested Caco-2 cells with the Quick-RNA Miniprep kit (Zymo Research) following manufacturer's protocol. cDNA was generated with the LunaScript RT Supermix (New England Biolabs), and SYBR Green based qPCR assays were run on ABI Prism 7000 Sequence Detection System using Luna Universal qPCR Mastermix (New England Biolabs) essentially as described [28]. The sequences of used qPCR primers are listed in the **Supplementary Table S2**. All qPCR tests were run in triplicate, and specificity of each amplification was assessed by the melting curve analysis of amplified samples. The expression of each profiled cytokine was normalized to the endogenous level of GAPDH reference [29].

Data analyses.

All statistical and multivariate analyses were carried out in R, Python, and Matlab [30]. Multivariate ordination analyses included principal components analysis (PCA) and phylogenetic UniFrac distance-based principal coordinates analysis (UF-PCoA). Where shown, statistical significance of group separation in ordination space was based on the permutation of the Davies-Bouldin index as we described previously [31]. Logistic regression with Lasso regularization (C=1) was run in ORANGE to reveal genera statistically associated with WM and YEM+ASP microbial communities as we did previously [29]. PICRUSt2 and STAMP software were used to evaluate the predicted encoded functions of profiled microbial communities [32]. Statistical significance of the differential pathway abundances between groups was calculated with the Welch's t-test with Benjamini-Hochberg correction for multiple hypothesis testing [33]. Pathway was defined as differentially encoded (DE) if it was at least 1.5-fold more prominent in either WM or YEM+ASP communities at the $\alpha \leq 0.01$ significance level. Unless stated otherwise, statistical significance of the differences in measured values among vessels or media was calculated with repeated measures ANOVA (RM ANOVA).

Results

Microbial fermentation of digested asparagus powder.

Dried asparagus powder was first subjected to the three-step digestion procedure (shown in **Figure 1A**) designed to simulate the human oro-gastro-intestinal digestion. The HGS system was then used to carry out a three-phase cultivation of human gut microbiota following a procedure outlined in **Figure 1B**.

Western diet medium represented the food digest entering colon in a subject consuming a typical Western diet (relatively high in animal proteins and fats). In the second phase, the medium was switched to the basal yeast extract medium supplemented with digested asparagus powder. Phase three was a control medium only containing yeast extract, vitamins, and salts (see **Table 1**). This combination of three phases of HGS operation allowed us to (i) compare community fermentation of nutrients obtained from the western diet vs digested asparagus powder, and to (ii) separate the specific effects of ASP fermentation from those arising due to the lack of western diet nutrients.

Two independent runs showed a good concordance in community density levels and changes upon medium switches (**Figure 2A**). During phase 1 (days 0-14), cell densities in all three vessels increased gradually as the seeded communities adapted and maximized the use of WM components. The overall density decreased from proximal to transverse to distal vessels (see distal vessel panel of **Figure 2A**), likely due to the diminishing nutrient availability as was observed in other HGS runs [18, 20]. Switching to YEM+ASP medium during phase 2 (days 15-28) lowered cell densities in all three vessels, suggesting a potential growth restriction of the ASP medium. Since the total amount of macronutrients was equal between the WM and YEM+ASP media, this reduction in cell density may be attributed to either (i) the poorer accessibility of nutrients in YEM+ASP or (ii) the previously documented presence of antimicrobial phytochemicals in asparagus including polyphenols, saponins, and alkaloids [1]. Interestingly, cell density in the transverse vessel gradually exceeded that of the proximal vessel during phase 2, consistent with the presence of a significant amount of dietary fiber in the YEM+ASP medium requiring longer fermentation times and thus providing more nutrients to the transverse vessel communities. Note that fresh medium is directly added to the proximal vessel only, which usually maintains the densest microbial communities due to higher nutrient availability [18, 20]. Hence, our observation presents a notable diet associated shift in the dominant colonic region of microbial activity. Switching to YEM during phase 3 (days 29-42) lowered the cell densities drastically across all three HGS vessels due to the limited nutritional value of YEM (**Figure 2A**).

Asparagus fermentation causes a shift in microbial community structure.

In contrast to the reduction in cell densities between WM and YEM+ASP cultures, community diversity increased upon this medium switch (**Figure 2B**). Community evenness was more comparable, only reaching the statistically significant increase in the proximal vessel. YEM communities had noticeably higher evenness in all three vessels, attributed to the reduction in the abundance of dominant community members in the nutrient-poor environment.

At the class level, WM and YEM+ASP communities were dominated by classes Clostridia, Bacteroidia, and Negativicutes (**Figure 2C**). Switching the supplied medium from WM to YEM+ASP led to a statistically significant reduction in cell counts of Negativicutes in the proximal vessel and Bacteroidia in the distal vessel; total Deltaproteobacteria increased instead on YEM+ASP in the proximal ($p<0.04$) and distal ($p=0.09$) vessels. Because class Deltaproteobacteria is known to house several detrimental members of human gut microbiota, we calculated the total counts of presumed beneficial and presumed detrimental members in each sample. As shown in **Figure 2D**, the counts of beneficial members were comparable between WM and YEM+ASP cultures; however, the numbers of potentially detrimental microbes were higher in cultures provided the digested asparagus powder. YEM medium shifted the beneficial-to-detrimental microbe ratio drastically towards the detrimental side.

At the genus level, microbiota abundances were less consistent across the three vessels. *Bacteroides*, *Faecalibacterium*, *Mitsuokella*, *Phocaeicola*, and *Ruminococcus* were overall the most abundant genera (see **Supplementary Table S1**). These differences were sufficiently large to separate samples in PCoA ordination space according to the supplied medium ($p<0.001$) as shown in **Figure 3A**.

To identify the key members of microbial communities that were predictive of these medium-based differences in each vessel, we employed a logistic regression based discriminant analysis [29]. This analysis revealed microbial genera that were uniquely associated with a microbial community of each medium (**Figure 4** shows the top discriminating genera for WM and YEM+ASP media). The genera that were abundant on the Western pattern diet medium but were not competitive on the asparagus digest included *Mitsuokella* (class Negativicutes) in the proximal vessel, *Mitsuokella*, *Negativibacillus*, and *Eisenbergiella* (both Clostridia) in the transverse vessel, and *Negativibacillus*, *Eisenbergiella*, and phylotypes classified as *Ruminococcus2* (from family Lachnospiraceae in the class Clostridia) in the distal vessel. It is likely that these members of the gut community failed to utilize asparagus digest as a source of nutrients or survive using microbial cross-feeding during the YEM+ASP phase. It could also be speculated that these members might have been affected severely by asparagus phytochemicals as described above, compared to other members of the community, resulting in a significant reduction of their abundances (**Figure 4** top row panels).

Genera that showed significant expansion in the YEM+ASP environment included *Ruminococcus* from family Ruminococcaceae (class Clostridia) in the proximal vessel, *Hungatella* (class Clostridia), *Marseilla* (class Bacteroidia), *Bilophila*, *Desulfovibrio* (both from class *Deltaproteobacteria*), and unidentified members of family Lachnospiraceae in the transverse vessel, as well as *Bilophila* and *Beduinibacterium* (class Clostridia) in the distal vessel (**Figure 4** bottom row panels). Because the counts of all of these genera were only increased in the presence of asparagus

digest (they were low in both WM and YEM media, see **Figure 4**), their expansion was due to the presence of favored nutrients among the digested ASP components.

Metabolite and antioxidant production vary among the growth media.

We measured concentrations of six short-chain fatty acids - acetate, propionate, butyrate, isovalerate, lactate, and succinate – in all profiled HGS samples. As expected, acetate was the most abundant SCFA, followed by propionate and butyrate. The total amount of measured SCFAs as well as the concentrations of individual fatty acids were generally comparable between the WM and YEM+ASP cultures (see a heatmap in **Figure 3B**). The switch from the WM to YEM+ASP medium led to a modest reduction on the amount of produced SCFAs in the proximal vessel (from 66.3mM to 62.8mM), concomitant with an increase in production in the transverse vessel (from 64.0mM to 73.2mM). This observation is consistent with the higher cell densities measured in the transverse vessel during phase 2, suggesting a relatively high metabolism in transverse vessel on the YEM+ASP medium. For all three vessels, YEM showed a drastic reduction in the total SCFA production as expected due to the limited nutrient availability during phase 3 (average total SCFA concentrations of 15mM,13mM and 16mM for proximal, transverse, and distal vessels, respectively). These similarities and differences were reflected in the distribution of samples in the SCFA concentration based PCA space (**Figure 3B**), with clear visible separation of YEM samples.

Antioxidant capacity increased from WM (average 3.1 mmol/L) to YEM+ASP (average 5.6 mmol/L) across all three vessels, and YEM cultures had the lowest antioxidant capacity (average 1.9 mmol/L) (**Figure 3C**). This observation of increased antioxidant capacity due to asparagus fermentation is also confirmed by previous studies that found asparagus to possess significant antioxidant properties [34]. Antioxidant concentration of the freshly prepared YEM+ASP medium was 2.0 mmol/L on average, indicating that microbial fermentation led to a 2.8-fold increase in the available antioxidants ($p<0.005$ for each vessel based on the two-sample T-test).

Predicted functional capacities separate WM and YEM+ASP communities.

By using the PICRUSt2 algorithm, we estimated the functional repertoire of community genomes in all profiled samples. These repertoires were sufficiently distinct to separate the WM, YEM+ASP, and YEM sample groups in the PCA ordination space with statistical significance (**Figure 5A**), and a number of differentially encoded pathways were revealed (**Figure 5B**). The relative abundances of several prominent pathways that differed between WM and YEM+ASP samples are displayed in **Figure 5C**.

Overall, the Western pattern diet medium supported fermentation pathways and the flux through the TCA cycle. The latter observation is possibly due to the higher amount of total fats in the WM providing higher availability of acetate. Inorganic metabolism and cofactor biosynthesis genes were encoded more frequently in the asparagus digest-grown cultures, consistent with the increase in *Desulfovibrio* abundance in these samples and likely associated with the presence of inorganic electron acceptors such as sulfate in asparagus [35]. Elevated capacity for methionine biosynthesis in asparagus-grown cultures (**Figure 5C**) might be attributed to the higher sulfurylation activity due to the presence of sulfur-containing compounds in asparagus [36]. This is corroborated by the increased abundance of the members of Deltaproteobacteria and Clostridia, both of which have been shown to contain genes for sulfurylation enzymes [36].

It has been previously observed that flavonoids and polyphenols can directly interact with cell wall peptidoglycans and inhibit the growth of certain bacteria including *Escherichia coli*, *Pseudomonas fluorescens*, and *Staphylococcus aureus* [37]. The high concentration of polyphenols and flavonoids in asparagus could thus be expected to elicit a similar effect, resulting in the reduction of predicted repertoire of peptidoglycan maturation genes observed during asparagus fermentation.

Supernatant from fermented asparagus cultures protects epithelial cells against DSS-induced damage and inflammation.

DSS treatment has been used in many *in vivo* and *in vitro* studies to simulate epithelial damage often observed in irritable bowel disease (IBD) and other gastrointestinal illnesses [38-40]. To assess whether microbiota-fermented asparagus might protect gut tissues against injury or inflammation, differentiated Caco-2 colorectal epithelial cancer cells were subjected to such DSS treatment alone or in combination with culture supernatants from select WM and YEM+ASP samples. A combination of acetate, butyrate, and propionate (ABP) in concentrations matching those measured in the YEM+ASP supernatant was used as a control. As can be observed in **Figure 6**, DSS addition to the apical side of Caco-2 layers led to a reduction in cell metabolic activity and epithelial barrier integrity (**Figure 6** panels **A** and **B**, respectively). Concurrent administration of culture supernatants from YEM+ASP samples (day 28) but not from WM samples (day 14) significantly reduced the deleterious effect of DSS on the epithelial cells. Similar protective effects were also observed for the fresh digested asparagus medium and ABP SCFA combination. While the metabolic activity in cells supplemented with DSS + day 28 supernatant, DSS + ASP medium, and DSS + ABP SCFAs treated Caco-2 samples did not differ from that of the control samples (**Figure 6A**), cell layer integrity was still reduced, but to a significantly lower extent when compared with the DSS only-treated cells (**Figure 6B**).

DSS has been shown previously to elevate the expression of several pro-inflammatory cytokines including IL-6, IL-10, IL-12, TNFα, and IFNγ, while sometime also being able to increase the expression of anti-inflammatory TGFβ [39, 41, 42]. We therefore measured the mRNA expression of IL-6, IL-12A, TNFα, and TGFβ2 variant genes in the control and treated Caco-2 cells. In our differentiated Caco-2 layers, DSS administration elevated the mRNA expression of IL-6, IL-12, and TNFα (**Figure 6C**). Co-administration of day 28 supernatants (YEM+ASP cultures) protected against DSS-increased expression of IL-6 and IL-12, but did not have an effect on the TNFα levels. In comparison, WM supernatants had a smaller positive effect on IL-6 and IL-12 expression and further increased TNFα mRNA levels. While DSS treatment alone had no effect on the mRNA expression of TGFβ variant in our Caco-2 system, addition of both day 14 and day 28 supernatants significantly elevated the expression of this anti-inflammatory mediator (see **Figure 6C**).

Discussion and Conclusions

In this study we investigated the changes of the gut microbial communities and metabolite production upon fermentation of digested asparagus. Overall, the revealed evidence pointed to the efficient fermentation of asparagus by human gut microbiota, with similar production of short chain fatty acids, fermentation end-products, in comparison with communities maintained on the Western pattern diet medium (see **Figure 3B**). Sole fermentation of asparagus could alter human gut microbiota community structure and change SCFA and antioxidant profiles. The highest SCFA production shifted on the YEM+ASP medium from the proximal to the transverse vessel, indicating that more time was needed to ferment asparagus components in comparison with WM. Antioxidant capacity was also increased on the YEM+ASP medium in all three vessels (see **Figure 3C**), attributed to the effect of microbial transformation of asparagus components (an average 2.8-fold increase in the available antioxidants after fermentation of the YEM+ASP medium).

While many members of gut microbiota adapted to asparagus fermentation with minimal changes, some members were positively or negatively influenced by the switch from the WM to YEM+ASP medium (see **Figure 4**). Asparagus promoted a significant expansion of *Ruminococcus* in the proximal vessel, a key genus of mammalian gut with well-known capabilities to degrade complex polysaccharides [43], an observation in line with the complexity of asparagus phytochemicals. Previous studies have shown that the abundance of *Ruminococcus* was positively correlated with lower endotoxemia and lower BMI [44], and members of this genus are able to elicit either pro- or anti-inflammatory effects based on the specific strain and the host physiology [43]. However, we also observed that asparagus fermentation favored the growth of sulfur-reducing members of the gut community

including *Bilophila* and *Desulfovibrio*. Members of these genera (e.g., *B. wadsworthia*, *D. piger*, and *D. desulfuricans*) can utilize sulfur containing compounds to produce H_2S and are generally considered detrimental to human health [45]. Asparagus is rich in sulfur containing compounds including asparagusic acid and asparaptine [2, 46]. It is likely that the presence of these molecules led to an increased availability of sulfur-rich compounds in the YEM+ASP medium, and they are subsequently metabolized by the sulfate-reducing bacteria in the anaerobic environment. In line with this, pathways of assimilatory sulfate reduction were encoded more frequently in the YEM+ASP communities (see **Figure 5C**). H_2S production by human microbiota has been associated with several ill effects such as colonic inflammation and cancer, though some recent studies have attested to the protective role of H_2S against oxidative stress in the gut mucosa [47].

Our most intriguing finding was uncovering the protective role of fermented asparagus supernatant against a DSS-induced epithelial injury (see **Figure 6**). Both the cell metabolic activity and epithelial barrier function were less affected by DSS stressor in the presence of YEM+ASP supernatant. This effect was stronger for YEM+ASP supernatant than that for the addition of (i) fermented WM supernatant, (ii) fresh unfermented asparagus medium, or (iii) the solution of ABP short-chain fatty acids, possibly due to the elevated presence of antioxidants in the YEM+ASP medium [48]. Furthermore, YEM+ASP supernatant also reduced the DSS-induced expression of pro-inflammatory cytokines IL-6 and IL-12, while it increased the expression of anti-inflammatory TGFβ (see **Figure 6C**).

In conclusion, we present the first evidence of human gut microbial fermentation of raw asparagus. The beneficial effects of asparagus fermentation included an increase in antioxidant capacity, maintenance of SCFA production, and protection against epithelial injury and inflammation. The combination of these effects is expected to outweigh any potential negative outcome induced by the H_2S production.

Supplementary Materials

Supplementary Table S1: cumulative genus-level cell densities in all samples.

Supplementary Table S2: sequences of qPCR primers used in this study.

Acknowledgements

We are thankful to Michael Bottomley and Shamvabi Jha (both at Wright State University) for valuable comments. Work in O.P. laboratory was supported in part by NSF award DBI-1335772 and by Uprising Foods, Inc.

Author Contributions

Conceptualization, S.R. and O.P.; Methodology, S.R., B.B., B.N.P., D.R.C., and O.P.; Validation, B.B., S.P.B., and D.R.C.; Formal Analysis, S.R., and O.P.; Data Curation, S.R., S.P.B., and O.P.; Writing, S.R. and O.P.; Supervision, J.A.R.H., K.J.C., and O.P.; Project Administration, O.P.; Funding Acquisition, O.P.

Conflicts of Interest

The authors declare no conflict of interest.

References

1. Q. Guo, N. Wang, H. Liu, Z. Li, L. Lu and C. Wang, The bioactive compounds and biological functions of Asparagus officinalis L. – A review, *Journal of Functional Foods*, 2020, **65**, 103727.
2. E. Pegiou, R. Mumm, P. Acharya, R. C. H. de Vos and R. D. Hall, Green and White Asparagus (Asparagus officinalis): A Source of Developmental, Chemical and Urinary Intrigue, *Metabolites*, 2020, **10**, 17.
3. J. Kobus-Cisowska, D. Szymanowska, O. M. Szczepaniak, A. Gramza-Michałowska, D. Kmiecik, B. Kulczyński, P. Szulc and P. Górnaś, Composition of polyphenols of asparagus spears (Asparagus officinalis) and their antioxidant potential, *Ciência Rural*, 2019, **49**, e20180863.
4. Y.-P. Guo, L. Shao, M.-Y. Chen, R.-F. Qiao, W. Zhang, J.-B. Yuan and W.-H. Huang, In Vivo Metabolic Profiles of Panax notoginseng Saponins Mediated by Gut Microbiota in Rats, *Journal of agricultural and food chemistry*, 2020, **68**, 6835-6844.
5. M. Sanae and A. Yasuo, Green Asparagus (Asparagus officinalis) Prevented Hypertension by an Inhibitory Effect on Angiotensin-Converting Enzyme Activity in the Kidney of Spontaneously Hypertensive Rats, *Journal of agricultural and food chemistry*, 2013, **61**, 5520-5525.
6. A. Redondo-Cuenca, A. García-Alonso, R. Rodríguez-Arcos, I. Castro, C. Alba, J. Miguel Rodríguez and I. Goñi, Nutritional composition of green asparagus (Asparagus officinalis L.), edible part and by-products, and assessment of their effect on the growth of human gut-associated bacteria, *Food Research International*, 2023, **163**, 112284.
7. J. Zhao, W. Zhang, X. Zhu, D. Zhao, K. Wang, R. Wang and W. Qu, The aqueous extract of Asparagus officinalis L. by-product exerts hypoglycaemic activity in streptozotocin-induced diabetic rats, *Journal of the science of food and agriculture*, 2011, **91**, 2095-2099.
8. F. G. Elsaid, A. A. Shati and M. A. Sarhan, Role of Matricaria recutita L. and Asparagus officinalis L. against the neurotoxicity of diazinon in rats, *The Journal of Basic & Applied Zoology*, 2015, **72**, 26-35.
9. S. A. Sullivan, A. Q. M. Tran, G. Xu, Y. Yin, C. Zhou and V. L. Bae-Jump, Asparagus polysaccharide inhibits cell proliferation, adhesion and invasion in endometrial cancer cells, *Gynecologic Oncology*, 2017, **145**, 133.

10. T. S. Kahlon, M. H. Chapman and G. E. Smith, In vitro binding of bile acids by okra, beets, asparagus, eggplant, turnips, green beans, carrots, and cauliflower, *Food Chemistry*, 2007, **103**, 676-680.
11. Y. Huang, Q. Zhou, J. An, W. Cai and W. Lyu, Effect of Instant Asparagus Powder on Sleeping Disorder, *Agricultural Science & Technology*, 2017, **18**, 975-978,1001.
12. J. Kobus-Cisowska, E. Flaczyk, D. Kmiecik, A. Gramza-Michalowska, B. Kulczynski and P. Juszczak, Applicability of asparagus (Asparagus officinalis L.) as a component of meatloaf, *Nauka Przyroda Technologie. Uniwersytet Przyrodniczy w Poznaniu*, 2017, **11**, 87-96.
13. P. Solhi, S. Azadmard-Damirchi, J. Hesari and H. Hamishehkar, Effect of fortification with asparagus powder on the qualitative properties of processed cheese, *Int J Dairy Technol*, 2020, **73**, 226-233.
14. T. Sanz, A. Salvador, A. Jiménez and S. M. Fiszman, Yogurt enrichment with functional asparagus fibre. Effect of fibre extraction method on rheological properties, colour, and sensory acceptance, *European Food Research and Technology*, 2008, **227**, 1515-1521.
15. A. C. P. Vital, C. Itoda, Y. S. Crepaldi, B. R. Saraiva and P. T. Matumoto-Pintro, Use of asparagus flour from non-commercial plants (residue) for functional pasta production: Asparagus flour for functional pasta production, *Journal of food science and technology*, 2020, **57**, 2926-2933.
16. S. Pérez-Burillo, S. Rajakaruna, S. Pastoriza, O. Paliy and J. Ángel Rufián-Henares, Bioactivity of food melanoidins is mediated by gut microbiota, *Food Chem*, 2020, **316**, 126309.
17. R. Agans, A. Gordon, D. L. Kramer, S. Perez-Burillo, J. A. Rufian-Henares and O. Paliy, Dietary Fatty Acids Sustain the Growth of the Human Gut Microbiota, *Appl Environ Microbiol*, 2018, **84**, e01525-01518.
18. K. L. Sprague, S. Rajakaruna, B. Bandow, N. Burchat, M. Bottomley, H. Sampath and O. Paliy, Gut Microbiota Fermentation of Digested Almond–Psyllium–Flax Seed-Based Artisan Bread Promotes Mediterranean Diet-Resembling Microbial Community, *Microorganisms*, 2024, **12**, 1189.
19. A. Brodkorb, L. Egger, M. Alminger, P. Alvito, R. Assunção, S. Ballance, T. Bohn, C. Bourlieu-Lacanal, R. Boutrou, F. Carrière, A. Clemente, M. Corredig, D. Dupont, C. Dufour, C. Edwards, M. Golding, S. Karakaya, B. Kirkhus, S. Le Feunteun, U. Lesmes, A. Macierzanka, A. R. Mackie, C. Martins, S. Marze, D. J. McClements, O. Ménard, M. Minekus, R. Portmann, C. N. Santos, I. Souchon, R. P. Singh, G. E. Vegarud, M. S. J. Wickham, W. Weitschies and I. Recio, INFOGEST static in vitro simulation of gastrointestinal food digestion, *Nat Protoc*, 2019, **14**, 991-1014.
20. S. Rajakaruna, S. Pérez-Burillo, D. L. Kramer, J. Á. Rufián-Henares and O. Paliy, Dietary Melanoidins from Biscuits and Bread Crust Alter the Structure and Short-Chain Fatty Acid Production of Human Gut Microbiota, *Microorganisms*, 2022, **10**, 1268.
21. S. Rajakaruna, S. Pérez-Burillo, J. Á. Rufián-Henares and O. Paliy, Human gut microbiota fermentation of cooked eggplant, garlic, and onion supports distinct microbial communities, *Food & Function*, 2024, **15**, 2751-2759.
22. M. F. Polz and C. M. Cavanaugh, Bias in template-to-product ratios in multitemplate PCR, *Appl Environ Microbiol*, 1998, **64**, 3724-3730.

23. S. Perez-Burillo, T. Mehta, A. Esteban-Munoz, S. Pastoriza, O. Paliy and J. Angel Rufian-Henares, Effect of in vitro digestion-fermentation on green and roasted coffee bioactivity: The role of the gut microbiota, *Food Chem*, 2019, **279**, 252-259.
24. J. G. Caporaso, J. Kuczynski, J. Stombaugh, K. Bittinger, F. D. Bushman, E. K. Costello, N. Fierer, A. G. Pena, J. K. Goodrich, J. I. Gordon, G. A. Huttley, S. T. Kelley, D. Knights, J. E. Koenig, R. E. Ley, C. A. Lozupone, D. McDonald, B. D. Muegge, M. Pirrung, J. Reeder, J. R. Sevinsky, P. J. Turnbaugh, W. A. Walters, J. Widmann, T. Yatsunenko, J. Zaneveld and R. Knight, QIIME allows analysis of high-throughput community sequencing data, *Nat Methods*, 2010, **7**, 335-336.
25. S. Rajakaruna, D. A. Freedman, A. R. Sehgal, X. Bui and O. Paliy, Diet quality and body mass indices show opposite associations with distal gut microbiota in a low-income cohort, *J. Food Sci. Technol.*, 2019, **4**, 846-851.
26. A. Delgado-Osorio, B. Navajas-Porras, S. Pérez-Burillo, D. Hinojosa-Nogueira, Á. Toledano-Marín, S. Pastoriza de la Cueva, O. Paliy and J. Á. Rufián-Henares, Cultivar and Harvest Time of Almonds Affect Their Antioxidant and Nutritional Profile through Gut Microbiota Modifications, *Antioxidants*, 2024, **13**, 84.
27. P. R. Kiela and F. K. Ghishan, Physiology of Intestinal Absorption and Secretion, *Best Practice & Research Clinical Gastroenterology*, 2016, **30**, 145-159.
28. L. Rigsbee, R. Agans, V. Shankar, H. Kenche, H. J. Khamis, S. Michail and O. Paliy, Quantitative profiling of gut microbiota of children with diarrhea-predominant Irritable Bowel Syndrome, *Am J Gastroenterol*, 2012, **107**, 1740–1751.
29. M. P. Craig, S. Rajakaruna, O. Paliy, M. Sajjad, S. Madhavan, N. Reddy, J. Zhang, M. Bottomley, S. Agrawal and M. P. Kadakia, Differential MicroRNA Signatures in the Pathogenesis of Barrett's Esophagus, *Clin Transl Gastroenterol*, 2020, **11**, e00125.
30. O. Paliy and V. Shankar, Application of multivariate statistical techniques in microbial ecology, *Mol Ecol*, 2016, **25**, 1032-1057.
31. V. Shankar, D. Homer, L. Rigsbee, H. J. Khamis, S. Michail, M. Raymer, N. V. Reo and O. Paliy, The networks of human gut microbe-metabolite associations are different between health and irritable bowel syndrome, *Isme J*, 2015, **9**, 1899-1903.
32. G. M. Douglas, V. J. Maffei, J. R. Zaneveld, S. N. Yurgel, J. R. Brown, C. M. Taylor, C. Huttenhower and M. G. I. Langille, PICRUSt2 for prediction of metagenome functions, *Nature biotechnology*, 2020, **38**, 685-688.
33. Y. Benjamini and Y. Hochberg, Controlling the False Discovery Rate - a practical and powerful approach to multiple testing, *J Roy Stat Soc B Met*, 1995, **57**, 289-300.
34. J. W. Lee, J. H. Lee, I. H. Yu, S. Gorinstein, J. H. Bae and Y. G. Ku, Bioactive Compounds, Antioxidant and Binding Activities and Spear Yield of Asparagus officinalis L, *Plant Foods for Human Nutrition*, 2014, **69**, 175-181.
35. Y. Matsubayashi and Y. Sakagami, Phytosulfokine, sulfated peptides that induce the proliferation of single mesophyll cells of Asparagus officinalis L, *Proceedings of the National Academy of Sciences*, 1996, **93**, 7623-7627.
36. M. P. Ferla and W. M. Patrick, Bacterial methionine biosynthesis, *Microbiology*, 2014, **160**, 1571-1584.

37. M. Makarewicz, I. Drożdż, T. Tarko and A. Duda-Chodak, The Interactions between Polyphenols and Microorganisms, Especially Gut Microbiota, *Antioxidants*, 2021, **10**, 188.
38. B. Chassaing, J. D. Aitken, M. Malleshappa and M. Vijay-Kumar, Dextran sulfate sodium (DSS)-induced colitis in mice, *Curr Protoc Immunol*, 2014, **104**, 15.25.11-14.
39. Y. Araki, H. Sugihara and T. Hattori, In vitro effects of dextran sulfate sodium on a Caco-2 cell line and plausible mechanisms for dextran sulfate sodium-induced colitis, *Oncol Rep*, 2006, **16**, 1357-1362.
40. M. Roselli, A. Maruszak, R. Grimaldi, L. Harthoorn and A. Finamore, Galactooligosaccharide Treatment Alleviates DSS-Induced Colonic Inflammation in Caco-2 Cell Model, *Frontiers in Nutrition*, 2022, **9**.
41. P. Alex, N. C. Zachos, T. Nguyen, L. Gonzales, T. E. Chen, L. S. Conklin, M. Centola and X. Li, Distinct cytokine patterns identified from multiplex profiles of murine DSS and TNBS-induced colitis, *Inflammatory bowel diseases*, 2009, **15**, 341-352.
42. M. Toutounji, D. Wanes, M. El-Harakeh, M. El-Sabban, S. Rizk and H. Y. Naim, Dextran Sodium Sulfate-Induced Impairment of Protein Trafficking and Alterations in Membrane Composition in Intestinal Caco-2 Cell Line, *International Journal of Molecular Sciences*, 2020, **21**, 2726.
43. E. H. Crost, E. Coletto, A. Bell and N. Juge, Ruminococcus gnavus: friend or foe for human health, *FEMS Microbiology Reviews*, 2023, **47**, 1-23.
44. F. Salas-Perez, T. S. Assmann, O. Ramos-Lopez, J. A. Martínez, J. I. Riezu-Boj and F. I. Milagro, Crosstalk between Gut Microbiota and Epigenetic Markers in Obesity Development: Relationship between Ruminococcus, BMI, and MACROD2/SEL1L2 Methylation, *Nutrients*, 2023, **15**, 1550.
45. S. B. Singh, A. Carroll-Portillo and H. C. Lin, Desulfovibrio in the Gut: The Enemy within?, *Microorganisms*, 2023, **11**, 1772.
46. S. C. Mitchell and R. H. Waring, Asparagusic acid, *Phytochemistry*, 2014, **97**, 5-10.
47. D. Yonezawa, F. Sekiguchi, M. Miyamoto, E. Taniguchi, M. Honjo, T. Masuko, H. Nishikawa and A. Kawabata, A protective role of hydrogen sulfide against oxidative stress in rat gastric mucosal epithelium, *Toxicology*, 2007, **241**, 11-18.
48. J. Su, X. Zhang, Q. Kan and X. Chu, Antioxidant Activity of Acanthopanax senticosus Flavonoids in H2O2-Induced RAW 264.7 Cells and DSS-Induced Colitis in Mice, *Molecules*, 2022, **27**, 2872.
49. R. Caspi, R. Billington, I. M. Keseler, A. Kothari, M. Krummenacker, P. E. Midford, W. K. Ong, S. Paley, P. Subhraveti and P. D. Karp, The MetaCyc database of metabolic pathways and enzymes - a 2019 update, *Nucleic acids research*, 2020, **48**, D445-453.

Tables

Table 1. Medium composition, g l^{-1}

Medium component	*WM* *	*YEM + ASP* *	*YEM* *

Digested asparagus powder			
Pellet (dry residue) †	-	23.9	-
Digest supernatant ‡	-	29.7	-
Carbohydrates			
Arabinogalactan	1.8	-	-
Guar gum	0.9	-	-
Inulin	0.9	-	-
Pectin	1.8	-	-
Starch	4.4	-	-
Xylan	0.9	-	-
Cellobiose	0.9	-	-
Glucose	0.5	-	-
Fructose	0.5	-	-
Proteins			
Peptone	3.3	-	-
Casein	2.0	-	-
Lipids			
Palmitic acid	1.5	-	-
Stearic acid	0.8		
Mucin	*4.0*	-	-
Yeast extract	*3.0*	*3.0*	*3.0*
Vitamins	*1.0*	*1.0*	*1.0*
Salts, other components	*14.1*	*14.1*	*14.1*
Bile salts	0.2	0.2 **	0.1
Pancreatin	0.1	0.1 **	0.1

* WM – Western pattern diet medium, YEM+ASP – digested asparagus based medium, YEM – yeast extract medium

† Calculated wet weight equivalent: 145.8 g per liter of the medium

‡ Wet weight, represents 10% of the total digestion supernatant

** Amounts added during oro-gastro-intestinal digestion

626

627 **Figure legends**

628

629 **Figure 1. Experimental design.** Panel (**A**) depicts the steps of the *in vitro* oro-gastro-intestinal
630 digestion of asparagus powder. Panel (**B**) visualizes longitudinal design of the *in vitro* Human Gut
631 Simulator runs. Sample collection time points are indicated by a sample tube, and the analyses that were
632 performed on each collected sample are listed. The medium was switched from a standard Western diet
633 medium (WM) to the asparagus digest mixed with yeast extract and salts (YEM+ASP) after taking
634 samples at the end of day 14, and then again to the yeast extract medium (YEM) at the end of day 28.

635

636 **Figure 2. Dynamic changes in community density and composition.** Different columns represent data
637 for the three consecutively linked vessels simulating proximal, transverse, and distal colon as shown.
638 Panel (**A**) displays the cell density in each vessel. Panel (**B**) visualizes the calculated average community
639 diversity and evenness in the profiled samples as shown. Panel (**C**) shows the cumulative cell density of
640 different microbial classes at each time point; each column represents the average class density among
641 two replicate runs. Classes are grouped by their phylum assignment. Stars denote classes that had
642 statistically significant differential abundance between WM and YEM+ASP samples; **: $p < 0.01$, *: p
643 < 0.05 (RM ANOVA). Combined relative abundances of the designated beneficial and detrimental
644 microbes are plotted in panel (**D**). Where shown, error bars represent the standard error of the mean
645 (n=2), and statistical significance between WM and YEM+ASP samples is presented for comparisons
646 exceeding the α=0.05 level. The differences between WM/YEM+ASP and YEM communities were not
647 statistically tested.

648

649 **Figure 3. Analysis of microbial community composition and activity.** Panel (**A**) displays the output
650 of the unconstrained weighted UniFrac distance-based principal coordinates analysis (UF-PCoA) of the
651 genus abundance dataset. Panel (**B**) visualizes the concentrations of measured short-chain fatty acids in
652 all samples. In a heatmap, each column represents an average concentration of a particular acid among
653 the two replicate runs. PCA ordination analysis of the SCFA concentration dataset is shown on the right
654 side of panel (**B**). The percent of dataset variability explained by each axis in PCoA and PCA analyses is
655 shown in parentheses in axis titles. P values indicate the significance of group separation, NS - not
656 significant at the α=0.05 level. Panel (**C**) displays the changes in the average antioxidant capacity of
657 cultures over time. Error bars represent the standard error of the mean (n=2).

658

659 **Figure 4. Changes in the cell densities of genera discriminating WM and YEM+ASP communities.**
660 Discriminating genera were determined with logistic regression based discriminant analysis. Top row
661 displays changes in the average abundance of WM-discriminating genera in each vessel over time;
662 bottom row shows YEM+ASP discriminating genera. Note the differences in the Y axis scale among
663 panels and the break in the scale in top middle panel. Error bars represent the standard error of the mean
664 (n=2).

665

666 **Figure 5. Analysis of predicted functional capacities of microbial communities.** Panel (**A**) visualizes
667 the distribution of samples in the PCA ordination space based on the abundances of predicted
668 metagenome-encoded microbial functions. The percent of dataset variability explained by each axis is
669 shown in parentheses in axis titles. Panel (**B**) displays the numbers of statistically differentially encoded
670 (DE) pathways in the predicted metagenomes of the WM and YEM+bread maintained communities.
671 Predicted functional genes were assigned to pathways and pathway groups based on MetaCyc database
672 [49]. Only pathway groups with at least two DE pathways are shown. The relative prevalence of several
673 such pathways among WM and YEM+ASP samples is shown in panel (**C**) as box-and-whisker plots. P
674 values represent statistical significance (Welch's t-test) of the difference in pathway fraction between
675 WM and YEM+ASP sample sets.

676

677 **Figure 6. Effect of HGS culture supernatant and YEM+ASP medium on epithelial cell lines.** After
678 differentiation on trans-well membrane support, confluent Caco-2 cell layers were subjected to the
679 addition of DSS alone or in combination with either a mix of pure short-chain fatty acids (SCFAs),
680 freshly prepared YEM+ASP medium, or supernatants (SN) from HGS cultures grown on WM (samples
681 from proximal vessel taken on day 14) or YEM+ASP (day 28) media. Control columns represent Caco-2
682 cells without any treatment. Panel (**A**) visualizes the epithelial cell metabolic activity in cells 24 hours
683 after treatments as measured by the MTS assay after one and three hours of incubation. Panel (**B**)
684 displays changes in epithelial layer integrity six and 24 hours post-treatment in comparison to pre-
685 treatment values as measured by the TEER assay. Each column represents an average value among four
686 tests (samples from two runs ran in duplicate), and error bar shows the standard error of the mean (n=4).
687 Statistical significance was determined with paired-samples one-tail T test. In panel (B), all DSS treated
688 samples reduced epithelial integrity compared to the changes in the control wells ($p < 0.01$, denoted with
689 **). Panel (**C**) shows the changes in the expression level of select inflammatory cytokines in Caco-2
690 cells 24 hours after treatments in comparison with the control wells. Shown values represent expression

691 ratios between average ΔCt scores in the treated and control samples (n=3 in each set); error bars
692 represent the standard error of the mean. Statistical significance of the differences was tested with the
693 two-tail T-test at the α=0.05 level and the significant values are displayed.

The data supporting this article have been included as part of the Supplementary Information.

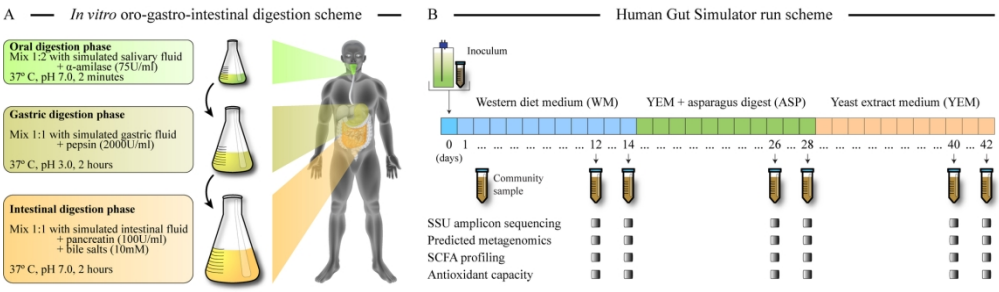

Figure 1

172x49mm (300 x 300 DPI)

Figure 2

172x171mm (300 x 300 DPI)

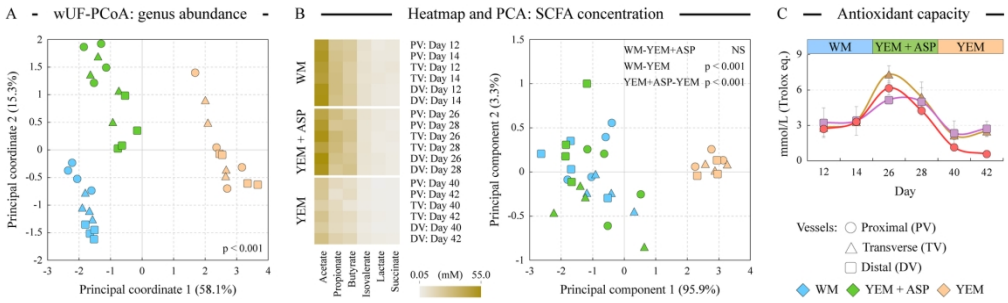

Figure 3

172x50mm (300 x 300 DPI)

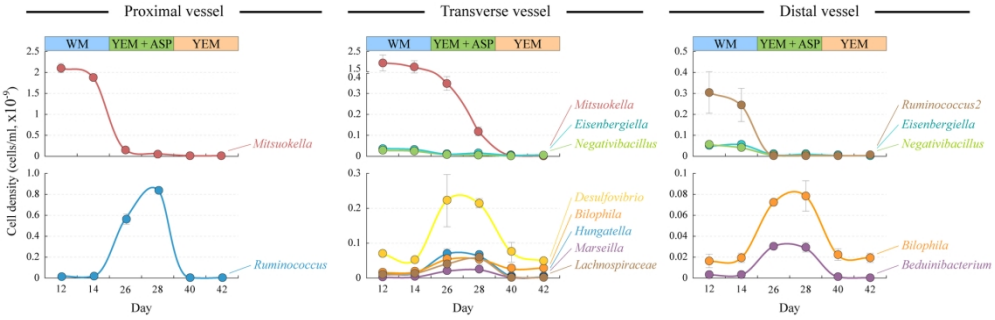

Figure 4

172x54mm (300 x 300 DPI)

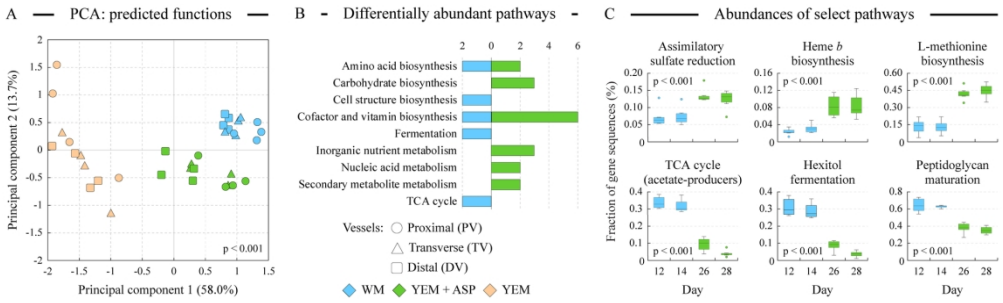

Figure 5

172x50mm (300 x 300 DPI)

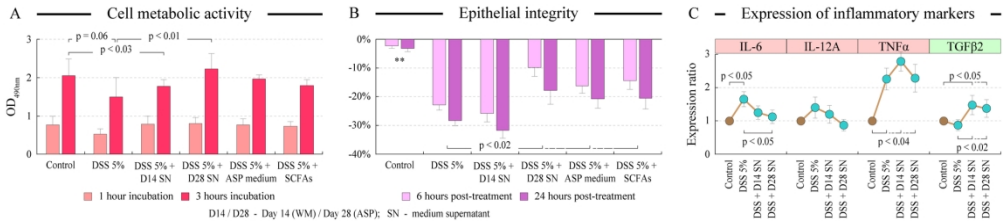

Figure 6

172x37mm (300 x 300 DPI)